Shocks in *n*-dodecane/nitrogen mixtures: a molecular dynamics study

Ethan S. Genter, Amitesh S. Jayaraman, Andrea Nobili, Hai Wang
Department of Mechanical Engineering, Stanford University
Stanford, CA 94305, USA

1 Introduction

Detonations involve interactions between fuel molecules and high-speed multi-component shock fronts ($M \sim 5-6$). These interactions determine the rate of pyrolysis and oxidation of the fuel that in turn influence the detonation cellular structure [1–3]. These interactions also involve energy and momentum transfers under non-equilibrium conditions. For instance, it has recently been shown that the large velocity gradients present in gaseous shocks generate a population of superheated molecules that are characteristic of the translational non-equilibrium in the shock region [4, 5]. Moreover, the gas immediately behind the shock is typically translationally hot but vibrationally cold [6]. While the influence of translational superheating and vibrational non-equilibrium on reaction kinetics in hydrogen-oxygen detonations was shown to be small [4, 6], the influence of translational and vibrational non-equilibrium in hydrocarbon fuel-air mixtures and the impact of rotational non-equilibrium of long-chain hydrocarbons in shocks, remain unexplored. Given that continuum simulations of gaseous detonations have conventionally relied on the assumption of local thermal equilibrium in modeling the impact of shock compression on chemistry, guidance in modeling sub-continuum scale phenomenon becomes critical to treating momentum and energy transfer in order to capture accurate, local reaction kinetics.

In this study, molecular dynamics (MD) simulations were used to investigate the impact of the large temperature and pressure gradients across shocks on the momentum and internal energy distribution of n-dodecane molecules passing through a nitrogen (N_2) shock front. Bifurcation in species concentration in the shock front was observed, where the N_2 concentration was found to peak ahead of n-dodecane. The bifurcation is the result of the disparate inertia that induces a significant drift velocity (~ 500 m/s) between n-dodecane and N_2. Immediately following a shock, n-dodecane molecules were found to be translationally hot, but vibrationally and rotationally cold, as expected. Analysis of molecular orientation reveals that the large temperature and pressure gradients in a $M = 5$ shock front freeze the molecular orientation within the shock as the angular velocity of the *n*-dodecane molecules vanishes. This would have implications in the kinetics and transport of long-chain hydrocarbons behind shocks.

2 Methods

2.1 Simulation Set-up

To probe the effect of large temperature and pressure gradients across shocks on the momentum and internal energy distribution of n-dodecane, two types of MD simulations were performed for mixtures of

Correspondence to: egenter@stanford.edu

dilute n-dodecane in N_2. Simulation I considered a shock traveling through a uniform, multi-component mixture of N_2 and n-dodecane (with mole fractions $X_{N_2} = 88/89$ and $X_{C_{12}H_{26}} = 1/89$), and Simulation II considered a pure N_2 shock impacting nine n-dodecane molecules. In both simulations, the pre-shock pressure and temperature were chosen to be $P_a = 5$ atm and $T_a = 300$ K, where the subscript a denotes the pre-shock state.

All MD simulations were performed using LAMMPS [7] with the Velocity-Verlet integrator. The bonded and non-bonded parameters for n-dodecane were modeled using the L-OPLS potential [8]. Intermolecular Lennard-Jones (L-J) interactions for N_2 were modeled using the parameters from Bouanich [9]. N_2 was modeled to be fully vibrationally excited with harmonic bond frequencies matching the vibrational data from Irikura [10]. All intermolecular interactions were modeled by a L-J 12-6 potential with a cut-off distance of 13 Å and a Coulombic pairwise interaction with a cut-off distance of 30 Å.

In Simulation I, the mixture was equilibrated at the pre-shock temperature T_a and pressure P_a in first a canonical and then a microcanonical ensemble for 100 ps each. Periodic boundary conditions were applied in the width-wise directions, and fixed, ideal, reflective walls, where collisions were specular-elastic, were applied in the length-wise direction. After equilibration, a piston moving at a constant speed U in the length-wise direction was introduced at one end of the box to produce a $M = 5$ shock.

Simulation II was conducted using two simulation boxes. The first box was prepared similar to that in Simulation I to produce a $M = 5$ shock in pure N_2. A second simulation box was filled with N_2 at T_a and P_a along with a single n-dodecane molecule. The gas was then equilibrated in an isothermal-isobaric ensemble for 5 ns. Following equilibration of the gas, a sphere of diameter 1.3λ, where λ is the pre-shock mean free path, centered at the center-of-mass of the n-dodecane molecule was extracted from the gas. To sample various orientations of the n-dodecane molecule, eight additional spheres were extracted from the same simulation box at eight different times. All spheres were then placed in uniformly separated holes of the same size cut from the pre-shock gas in the first simulation box. The simulation was run until all nine n-dodecane molecules had passed through the shock front and equilibrated with the post-shock gas at temperature T_b and velocity V_b. Simulation II was run eleven times, each with a unique set of initial n-dodecane molecules, with different orientations. Thermostatting and barostatting in all simulations was performed in the Nosé-Hoover style; a 1 fs timestep was used in all simulations.

2.2 Analysis

Both simulations provide insights into the mechanisms of non-equilibrium momentum and energy transfer between the gas shock and *n*-dodecane molecules. In order to capture non-equilibrium behavior, several quantities were determined as a function of location relative to the shock front. Simulation I, which captures behavior of a shock traveling through a multi-component gaseous mixture, was used to analyze the non-equilibrium momentum transfer process in the shock front. To this end, species concentrations and center-of-mass velocities were calculated for both n-dodecane and N_2 as a function of location, relative to the shock front. Species concentrations (n_i) are normalized with respect to the pre- (a) and post-shock (b) concentrations:

$$n_i^0 = \frac{n_i - n_{i,a}}{n_{i,b} - n_{i,a}}. \tag{1}$$

Simulation II, which captures the transient process of an N_2 shock impacting n-dodecane molecules, was used to analyze the non-equilibrium energy transfer process in the shock front. At a given location in the local gas frame of reference, n-dodecane and N_2 have molecular kinetic energy (E_i) composed of both translational ($E_{i,\text{trans}}$) and internal contributions ($E_{i,\text{int}}$). The kinetic energy contributions

can be converted to corresponding effective translational and internal temperatures by dividing them by $N_{\text{DOF}}Nk_B/2$, where N is the number molecules, N_{DOF} is the number of degrees of freedom per molecule associated with each kinetic energy term (equal to 3 for translational modes, 3 for N_2 internal modes, and 111 for n-dodecane internal modes) and k_B is the Boltzmann constant. We use the notation Θ to represent effective temperature, and if the gas is in local equilibrium, Θ would be the conventional temperature T. Θ may be normalized using Eq. 2 relative to pre- and post-shock temperatures:

$$\Theta^0_{i,\beta} = \frac{\Theta_{i,\beta} - T_{i,\beta,a}}{T_{i,\beta,b} - T_{i,\beta,a}}, \tag{2}$$

where $\beta =$ trans or int.

Lastly, molecular orientation of n-dodecane molecules was also analyzed. Here, molecular orientation is described by the angle θ between the vector that lies along the longest dimension of an n-dodecane molecule and a coordinate axis (i.e., x, y, or z), where z is the direction of shock propagation. The longest dimension of a molecule was determined instantaneously by the largest distance between any two atoms in the same molecule.

3 Results and Discussion

3.1 Momentum Transfer in the Shock Front

Fig. 1a shows the velocity profiles of n-dodecane and N_2 and the drift velocity (i.e., difference between the N_2 and n-dodecane velocity) within the $M = 5$ shock of thickness δ traveling through a uniform mixture of n-dodecane and N_2 (Simulation I). Following incoming gas from right to left, we can see that N_2 velocity rises more quickly than n-dodecane velocity upon interacting with the shock front and back (as defined by the blue dashed lines at $z/\delta = \pm 0.5$). Note that values of $z/\delta > 0.5$ denote the pre-shock region and values of $z/\delta < 0.5$ denote the post-shock region. The earlier acceleration of N_2 leads to a significant drift velocity between N_2 and n-dodecane whereby n-dodecane takes several (~ 5) mean free paths to catch up to the post-shock gas velocity. This is unlike the phenomenon observed in [4] where super-heated molecules were observed to 'surf' the shock front by repeatedly being accelerated far ahead of the shock, decelerated by the pre-shock gas, and then re-accelerated by the shock. Here, for a shock propagating in a dilute n-dodecane-N_2 mixture, the n-dodecane molecules do not surf but instead pass directly through the shock due to their larger inertia.

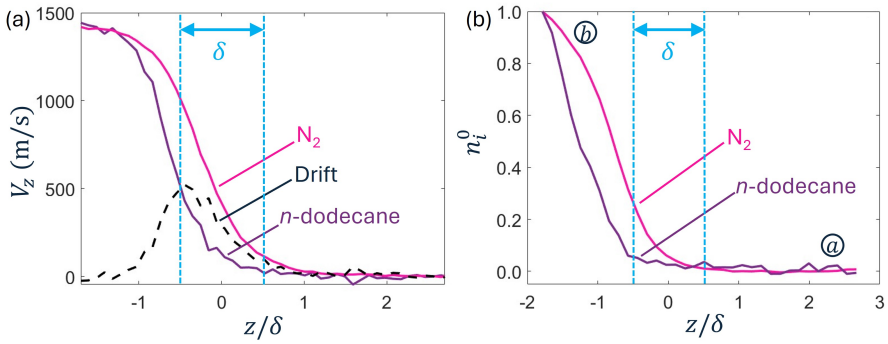

Figure 1: For a shock traveling left to right through a mixture of n-dodecane and N_2 (Simulation I). (a): z-direction velocity of N_2 and n-dodecane, and drift velocity, relative to the shock with shock thickness δ bracketed by the blue dashed lines. (b): concentration of n-dodecane and N_2 relative to the shock.

The significant drift velocity observed in Fig. 1a leads to a difference in species concentration profiles. Fig. 1b shows a species bifurcation, with n-dodecane concentration trailing behind N_2, consistent with results from [11] for xenon-oxygen-helium mixtures. In both cases, lighter species precede heavier species, causing a spatial bifurcation in species concentration. This is expected because the heavier species accommodates more slowly to the shock leading to a slower rise in its concentration. Additionally, the spatial species bifurcation can potentially explain the absence of the surfing phenomenon in n-dodecane as any super-heated n-dodecane molecules produced would necessarily come from the region of the n-dodecane layer within the shock and would have to first interact with the N_2 layers of the shock before reaching the shock front. The N_2 layers could therefore screen and slow down any n-dodecane molecules with the potential to surf.

3.2 Energy Transfer in the Shock Front

The differential momentum transfer between the gas and n-dodecane molecules observed in the shock front is also coupled to the energy transfer processes therein, through the large drift velocity and large temperature, pressure, and velocity gradients present in the shock; this can be seen in Fig. 2, which shows for a steady shock traveling through a uniform mixture of n-dodecane and N_2, species-specific profiles of translational temperature (panel a) and internal temperature (panel b), relative to the shock position. In both cases, the n-dodecane temperature lags behind that of N_2, consistent with the momentum transfer discussed in Sec. 3.1. We note in particular that the rise of both n-dodecane and N_2 translational temperature takes place ahead of the internal temperature rise (i.e., translational temperature peaks closer to the shock) indicating non-equilibrium energy transfer in the shock front where n-dodecane is translationally hot and internally (vibrationally and rotationally) cold.

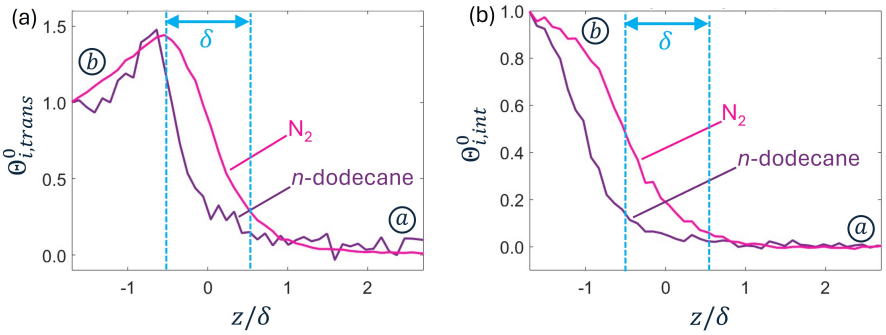

Figure 2: Shock traveling left to right through a mixture of n-dodecane and N_2 (Simulation I): (a) translational temperature of N_2 and n-dodecane relative to the shock of thickness δ bracketed by the blue dashed lines, and (b) internal temperature of N_2 and n-dodecane relative to the shock.

To investigate the internal energy distribution and rovibrational non-equilibrium in greater detail we analyze the orientation and rotational dynamics of n-dodecane within the shock. An ensemble of n-dodecane molecules is expected to span the full range of molecular orientations of $\Delta\theta = 180°$ under the equilibrium condition. Fig. 3a that shows $\Delta\theta$ along the three principal coordinates in the pre-shock region, within the shock, and in the post-shock region. While the $\Delta\theta$ value attained in the pre-shock and post-shock regions are clearly impacted by limited statistics, the figure clearly shows that within the shock, n-dodecane molecules have narrower ranges of orientation than those in the pre-shock and post-shock regions. The cause is demonstrated in Fig. 3b, which shows the time history of the molecular orientation of a selected n-dodecane molecule before, during and after shock passage. As it can be seen, the molecule undergoes nearly free, unhindered rotation albeit minor perturbations due to N_2 collisions

until it enters into the shock where its orientation becomes largely frozen. The molecule resumes free rotation as it leaves the shock front and enters into the post-shock gas. The maximum span of θ values gives rise to $\Delta\theta$ for each n-dodecane sampled. An average of $\Delta\theta$ over 100 individual n-dodecane time histories (i.e., over all simulations of type II) yields the average $\Delta\theta$ values presented in Fig. 3a.

The reduced range of molecular orientations is in fact expected. As an n-dodecane molecule enters into the shock, the front end of the molecule experiences a higher density, higher-kinetic energy N_2 gas than the tail end. This differential effectively yields a torque in the direction opposite to the angular momentum of the molecule. The effect of the torque is manifested as if the molecule "remembers" its orientation at the moment it enters the shock.

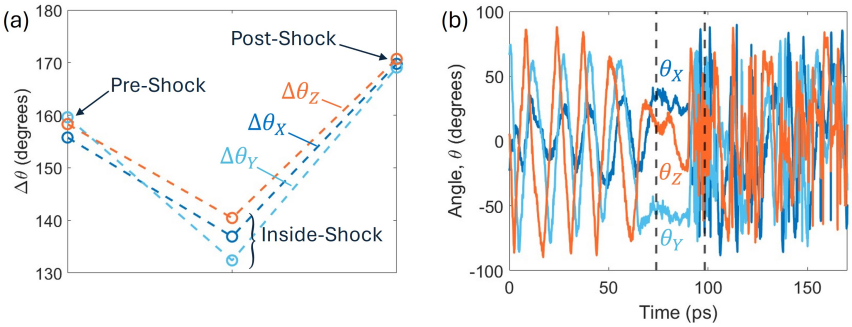

Figure 3: n-Dodecane molecules impacted by an N_2 shock (Simulation II): (a) average total change in n-dodecane molecular orientation $\Delta\theta$ prior to interacting with the shock (pre-shock), within the shock (inside-shock), and after passing through the shock (post-shock), and (b) time history of the molecular orientations of an n-dodecane molecule. In panel (b), the shock propagates from right to left; the two dashed lines bracket the time period during which the molecule is inside the shock.

While translational and rotational non-equilibrium do not persist beyond several mean free paths past the shock front, the current findings can have significant implications for chemical kinetics and molecular transport in continuum modeling of detonations. For instance, in the region of the shock, the non-equilibrium energy transfer and species concentration bifurcation can both modify kinetics through the modified energy distribution (i.e., non-Maxwell-Boltzmann distribution) and perturbed local number densities, respectively, all of which could lead to modified kinetic rates and potentially impact processes such as fuel pyrolysis. The observations of the concentration bifurcation and inter-species drag or drift impact continuum-level simulations where shocks are considered to transfer momentum and energy to all species simultaneously.

4 Conclusions

MD simulations of dilute, multi-component mixtures of N_2 and n-dodecane were performed to analyze the differential momentum transfer and non-equilibrium energy transfer in the shock front. The large velocity gradients in n-dodecane-N_2 shocks contribute to an inertial effect leading to a significant drift velocity between the heavier n-dodecane and the lighter N_2. The drift velocity causes a spatial bifurcation in their concentration immediately behind the shock front. Within the shock, n-dodecane is translationally hot and internally (rotationally and vibrationally) cold. During shock passage an effective torque is applied to n-dodecane that restricts the range of accessible molecular orientations, effectively freezing its orientation during shock passage.

5 Acknowledgments

The work was supported by Air Force Office of Scientific Research, United States under Grant FA9550-20-1-0398 managed by Dr. Chiping Li, and by the Office of Naval Research, United States under Grant N00014-22-1-2606 managed by Dr. Steven Martens. ESG acknowledges support by the National Science Foundation Graduate Research Fellowship under Grant No. DGE-1656518. Some of the computing for this project was performed on the Sherlock cluster at Stanford University. The authors thank Stanford University and the Stanford Research Computing Center for providing computational resources and support that contributed to these research results.

References

[1] P. A. Meagher, X. Shi, A. S. Jayaraman, N. Kateris, X. Zhao, and H. Wang, "The Hydrodynamic Origin of the Detonation Cell", In The 29th International Colloquium on the Dynamics of Explosions and Reactive Systems (ICDERS), SNU Siheung, Korea, 270 (2023).

[2] J. Crane, J. T. Lipkowicz, X. Shi, I. Wlokas, A. M. Kempf, and H. Wang, "Three-dimensional detonation structure and its response to confinement", Proc. Combust. Inst. 39 (3) (2023) 2915-2923.

[3] E. S. Genter, J. B. Kennedy, C. Sipper, A. S. Jayaraman, N. Montes, and H. Wang, "Regularity of detonation cellular structures in hydrocarbon mixtures of moderate effective activation energies", Proc. Combust. Inst. 40 (2024) 105744.

[4] A. S. Jayaraman, E. S. Genter, W. Dong, and H. Wang, "Collision enhancement in shocks and its implication on gas-phase detonations: A molecular dynamics and gas-kinetic theory study", Proc. Combust. Inst., 40 (1-4) (2024) 105741.

[5] R. Murugesan, and M. Radulescu. "The influence of non-equilibrium translational effects on reactive dynamics during shock to detonation transition using molecular dynamics", In The 29th International Colloquium on the Dynamics of Explosions and Reactive Systems (ICDERS), SNU Siheung, Korea, 274 (2023).

[6] X. Shi, A. S. Jayaraman, and H. Wang, "Probing vibrational nonequilibrium in detonations with ozone", Proc. Combust. Inst. 40 (1-4) (2024) 105695.

[7] A.P. Thompson, H.M. Aktulga, R. Berger, D.S. Bolintineanu, W.M. Brown, P.S. Crozier, P.J. In 't Veld, A. Kohlmeyer, S.G. Moore, T.D. Nguyen, R. Shan, M.J. Stevens, J. Tranchida, C. Trott, and S.J. Plimpton, "LAMMPS - a flexible simulation tool for particle-based materials modeling at the atomic, meso, and continuum scales", Comput. Phys. Commun. 271 (2022) 108171.

[8] S. W. I. Siu, K. Pluhackova, and R. A. Böckmann, "Optimization of the OPLS-AA force field for long hydrocarbons, J. Chem. Theory Comput. 8 (2012) 1459–1470.

[9] J.-P. Bouanich, "Site-site Lennard-Jones potential parameters for N_2, O_2, H_2, CO and CO_2, J. Quant. Spectrosc. Radiat. Transfer 47 (4) (1992) 243–250.

[10] K. K. Irikura, "Experimental Vibrational Zero-point Energies: Diatomic Molecules", J. Phys. Chem. Ref. Data 36 (2007) 389–397.

[11] S. V. Kulikov and G. B. Manelis, "The Effect of Small Xe Additives on the Detonation Threshold of an O_2—H_2—He Mixture", Dokl. Chem. 382 (2002).